TÜBİTAK

Turk J Elec Eng & Comp Sci, Vol.20, No.1, 2012, © TÜBİTAK
doi:10.3906/elk-1007-577

Reducing electromagnetic interferences in flyback AC-DC converters based on the frequency modulation technique

Gökhan ÇABUK[1], **Selçuk KILINÇ**[2,*]
[1] *Graduate School of Natural and Applied Sciences, Dokuz Eylül University, İzmir-TURKEY*
e-mail: gokhan.cabuk@yahoo.com
[2] *Department of Electrical and Electronics Engineering, Dokuz Eylül University, İzmir-TURKEY*
e-mail: selcuk.kilinc@deu.edu.tr

Received: 11.07.2010

Abstract

One of the most preferable types of switched-mode power supplies (SMPS) is the flyback converter, due to its wide range of application areas. Properties such as low cost, provision of multiple output voltage terminals, and higher efficiencies make it important, and hence its usage in technologies including cell phone chargers, personal computers, set-top boxes, and televisions is increasing. Special attention should be paid to the design of this type of converter due to its working principles and electromagnetic interference (EMI) performance. Rapid switching of high current and high voltage during the operation of SMPS causes an EMI problem. The level of the EMI noise should be reduced in order to not interfere with the operation of other equipment. One of the methods for mitigating EMI emissions is the frequency modulation (FM) technique. In this paper, the FM technique, which has been increasingly used as an EMI-reduction method in SMPS, is investigated. The modulation technique that was applied to the switching frequency of the flyback converter is analyzed and its effect on the EMI performance is discussed. The FM technique was tested on an AC-DC flyback converter prototype that was built with an L6566B integrated circuit. Conducted emission noises from the SMPS were measured using an EMI receiver. Experimental results showed that EMI levels were reduced after the application of the FM method.

Key Words: *Electromagnetic interference, switched-mode power supplies, AC-DC flyback converter, frequency modulation technique*

1. Introduction

AC-DC and DC-DC switched-mode power supplies (SMPS) are preferred in many systems due to their advantage of switching at higher frequencies. High-frequency switching reduces the size of the components and the weight

*Corresponding author: Department of Electrical and Electronics Engineering, Dokuz Eylül University, İzmir-TURKEY

of the transformer, and it increases efficiency in comparison with linear power supplies [1,2]. However, while switching the current on and off increases the efficiency, it also generates conducted and radiated electromagnetic interference (EMI) [3,4]. Generation of conducted and radiated EMI is an undesirable feature of these converters. If they are not mitigated, EMI currents and voltages can corrupt the power source to the converter and interfere with the operation of other adjacent equipment supplied by the same source [5]. They might constitute unexpected operating conditions for the equipment. In order to prevent this situation, EMI noise limits are determined for the converters. EMI noises of the designed converters must be within these limits as determined by regulatory institutions such as the International Special Committee on Radio Interference (CISPR).

Most pulse-width modulation (PWM) converters are designed to switch at a fixed frequency with a variable duty cycle. The main source of the EMI in power converters comes from switching the voltage and current [5], as mentioned above. Due to rapid switching of high current and high voltage, EMI is a serious problem in SMPS. The switching device in a power converter operating at high frequency leads to the generation of large dv/dt and di/dt signals. Rapid transient voltage and current changes during turn-on and turn-off operations are the main sources of conducted and radiated EMI. In other words, electrical transitions with sharp edges produce electromagnetic radiation. The sharp-edge transients contain most of the frequency components. The most significant contributions to the EMI spectrum are at the fundamental switching frequency and its harmonics [4].

The most common method used in the reduction of the conducted EMI is the low-pass filtering of the noises by the input capacitor and input EMI filter [5,6]. In this way, the EMI is mostly attenuated by the time it reaches the power source. However, most of the time, the filtering is not perfect, and it often leaves enough residual switching current noises to cause the system to exceed the EMI limits and fail conducted EMI tests [5].

Some EMI reduction methods have been presented in the literature [7-10]. Sigma-delta modulation has been proposed as an alternative switching technique to reduce conducted EMI in SMPS [7]. Active filters have been employed for EMI reduction and harmonic compensation [8]. The resonance technique has also been used for mitigating EMI in switching power converters [9]. Using soft switching methods allows for the reduction of conducted noise and, therefore, the zero-voltage switching and zero-current switching techniques have been employed in order to reduce EMI noises [10].

These approaches are important steps in dealing with the conducted EMI issue. One powerful method to reduce EMI is the frequency modulation (FM) technique [4,11-14], which modulates the switching signal and spreads the energy over a wider frequency range. In the FM technique, the energy of each harmonic is spread into a band of frequencies, giving a wider spectrum with lower amplitudes [4]. By using this method, the frequency of the switching signal is modulated and the EMI noise is reduced in SMPS.

In the present work, an AC-DC flyback converter with an L6566B integrated circuit [15] was built as a prototype. It has a dedicated FM pin, allowing the designer to modulate the switching frequency and thus making it possible to reduce the peak value of EMI by means of spreading the spectrum. In order to investigate the effects of FM parameters on the EMI performance, computer simulations were carried out. The realized flyback converter was tested in the laboratory by measuring its EMI performance using an EMI receiver. The FM scheme was compared with the standard fixed-frequency switching scheme, and their spectral performances showed that the FM technique provides better EMI suppression than the fixed-frequency case.

The paper is organized as follows. A brief FM theory is given in Section 2. The spectrum of an FM signal and MATLAB simulation results for different FM parameters are also presented in this section. Section 3 includes the operating principles of the flyback converter built with L6566B. In Section 4, the EMI performance

of the converter with and without FM is given, together with the experimental measurement results. Conclusions are drawn in Section 5.

2. Frequency modulation technique as an EMI reduction method

In SMPS, the switching elements are controlled by PWM signals. As an approximation, a PWM signal with a small change in its duty cycle can be considered as a square-wave signal, which includes the fundamental frequency and the multiples of the fundamental frequency in its spectrum. Since a square-wave signal can be expressed as a summation of an infinite number of sinusoids at the fundamental frequency and its harmonics, we can start our analysis with a sinusoidal modulated FM signal.

Let $m(t)$ be the modulating signal given by:

$$m(t) = A_m \cos(2\pi f_m t), \tag{1}$$

where A_m is the amplitude and f_m is the frequency of the modulating signal. Let $c(t)$ be the carrier signal given by:

$$c(t) = A_c \cos(2\pi f_c t), \tag{2}$$

where A_c is the amplitude and f_c is the frequency of the unmodulated carrier. The resulting FM signal, $s(t)$, can be expressed as [16]:

$$s(t) = A_c \cos\left[\theta_i(t)\right], \tag{3}$$

where $\theta_i(t)$ is the instantaneous angle of the modulated signal, given by:

$$\theta_i(t) = 2\pi f_c t + \phi(t). \tag{4}$$

Here, $\phi(t)$ is the time-dependent phase angle, which can be written as:

$$\phi(t) = 2\pi k_f \int_0^t m(t)dt, \tag{5}$$

where k_f is the modulation sensitivity factor expressed in Hz/V. The instantaneous frequency of the resulting FM signal is:

$$f_i(t) = f_c + k_f A_m \cos(2\pi f_m t) = f_c + \Delta f_c \cos(2\pi f_m t), \tag{6}$$

where Δf_c $(=k_f A_m)$ is the frequency deviation representing the maximum departure of the instantaneous frequency of the FM signal from the carrier frequency [16]. Therefore, the instantaneous angle of the modulated signal becomes:

$$\theta_i(t) = 2\pi f_c t + \frac{\Delta f_c}{f_m} \sin(2\pi f_m t). \tag{7}$$

The ratio of Δf_c to f_m is called the modulation index (β), given by:

$$\beta = \frac{\Delta f_c}{f_m}. \tag{8}$$

Therefore, using Eqs. (3), (7), and (8), the FM signal can be written as [16]:

$$s(t) = A_c \cos\left[2\pi f_c t + \beta \sin(2\pi f_m t)\right]. \tag{9}$$

Another parameter of the FM signal is the rate of modulation (δ), given by:

$$\delta = \frac{\Delta f_c}{f_c}. \tag{10}$$

According to Carson's rule [17], the bandwidth of the FM signal can be calculated by:

$$B = 2f_m(1+\beta) = 2(\Delta f_c + f_m). \tag{11}$$

Figure 1 shows the spectra of the unmodulated sinusoidal carrier and the FM signal together. As is seen, the bandwidth is spread around the carrier frequency into the band B with lower amplitude after the modulation. This is the main motivation for modulating the frequency of the PWM signal of the switching element for the purpose of mitigating the EMI in SMPS.

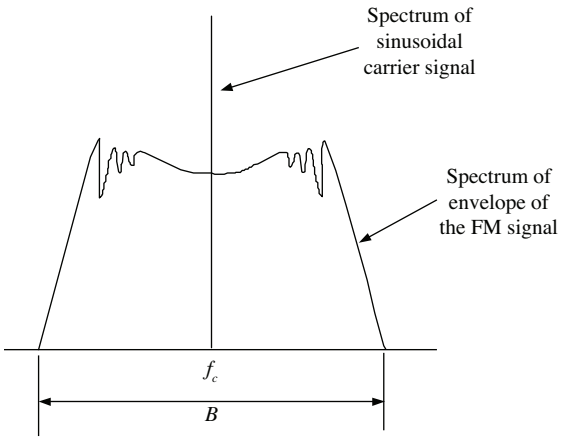

Figure 1. The effect of the FM on the spectrum of the sinusoidal waveform.

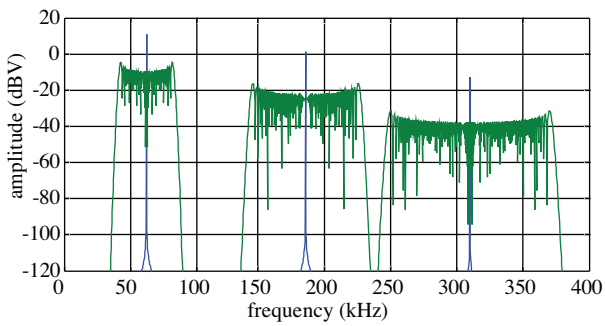

Figure 2. The spectra of a square-wave signal before and after modulation.

The spectrum of a square-wave signal contains components at the fundamental frequency and its harmonics, as mentioned above. Modulating the frequency of the square-wave signal should have the effect on the spectrum of spreading each individual harmonic into a certain frequency band. In order to test this, a MATLAB simulation was done, and the result was in agreement with the expectation [4], as seen in Figure 2.

The bandwidth of each harmonic, B_n, can be calculated by [4]:

$$B_n = 2f_m(1+n\beta). \tag{12}$$

Eq. (12) shows how the bandwidth of the harmonics increases as the number of harmonics gets higher. This may cause the spectrum to overlap at high frequencies, and hence reduce the efficiency of the FM technique.

Considering 2 successive spectra at the nth and $(n+1)$th harmonics, it is possible to determine the order of the harmonics at which overlap begins. With reference to Figure 3, for overlap to occur, the following condition should be satisfied.

$$nf_c + \frac{B_n}{2} = (n+1)f_c - \frac{B_{n+1}}{2} \tag{13}$$

Using Eqs. (12) and (13), the order of the harmonics at which overlap begins is found to be:

$$n_{overlap} = \frac{1}{2\delta} - \frac{1}{\beta} - \frac{1}{2}. \tag{14}$$

Overlap at very high frequencies is inevitable. However, its effect is not prevailing at these frequencies, since the magnitudes of these components are very small. Modulation parameters should be selected while taking into account Eq. (14) so as not to cause overlap at low frequencies.

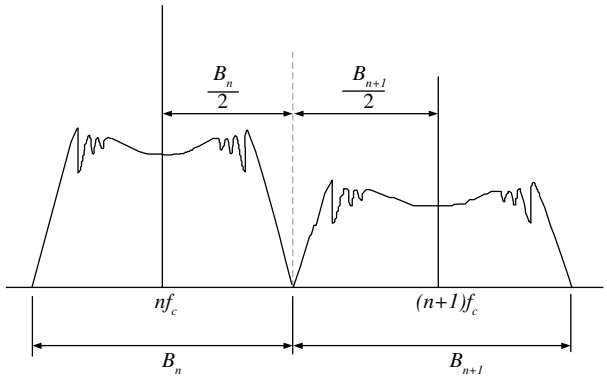

Figure 3. Spectrum for the harmonics at which overlap begins.

For efficient EMI noise reduction in the FM technique, the choices of the modulation parameters are important. Each parameter and its values should be selected and determined carefully for the designed system. One of the most important parameters for FM is the modulating signal. In order to investigate the effect of the modulating signal, 2 basic modulation profiles, triangular and sinusoidal, were studied. The frequency spectra of the signals modulated by these 2 profiles are shown in Figures 4-6, which were obtained by using MATLAB.

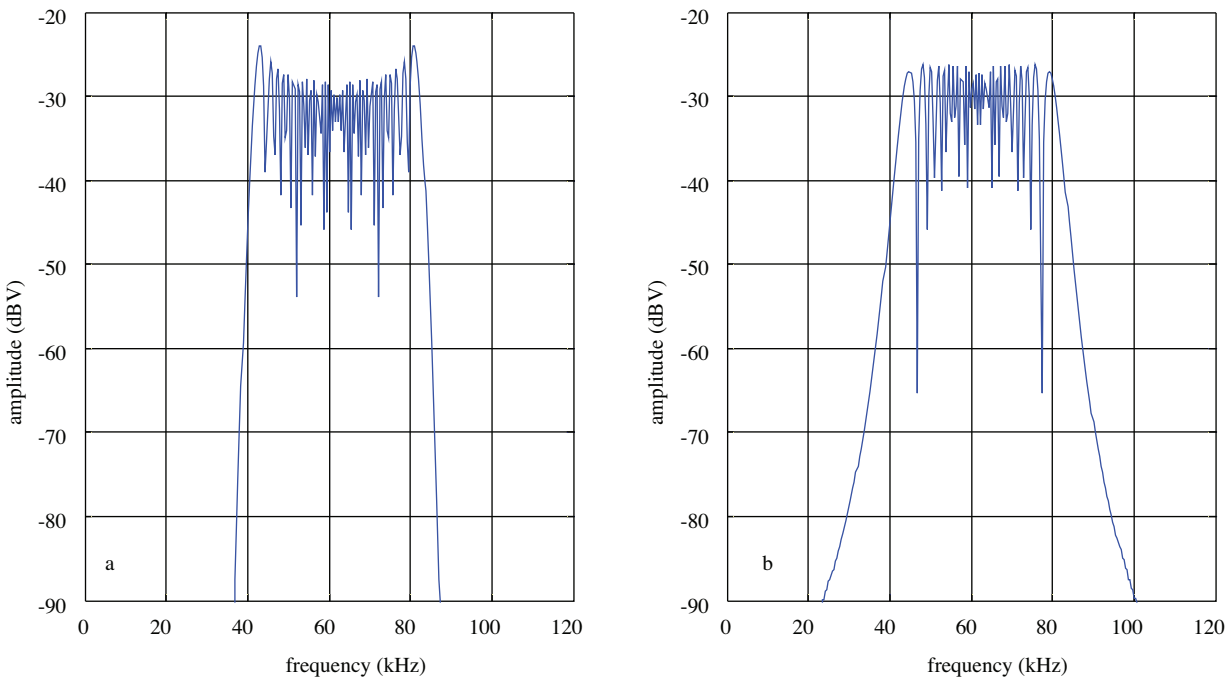

Figure 4. Spectra of FM signals modulated by a) sinusoidal and b) triangular profiles, f_c = 62 kHz, f_m = 375 Hz, Δf_c = 20 kHz.

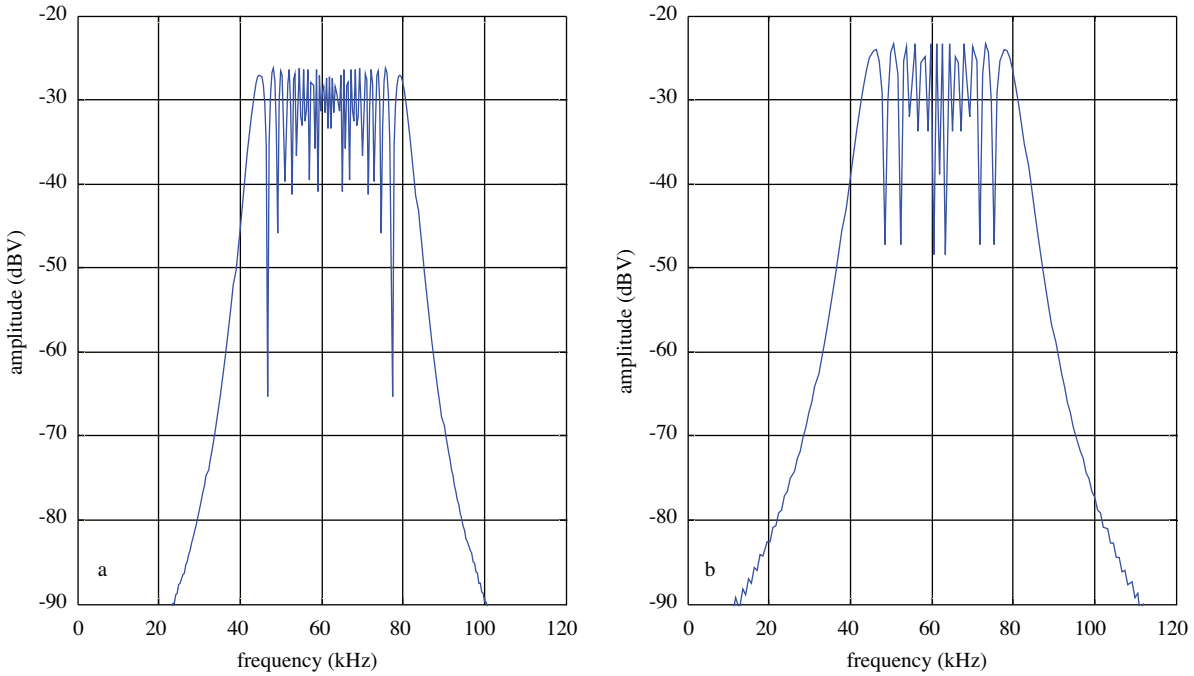

Figure 5. Spectra of FM signal modulated by triangular profile, $f_c = 62$ kHz, $\Delta f_c = 20$ kHz; a) $f_m = 375$ Hz, b) $f_m = 750$ Hz.

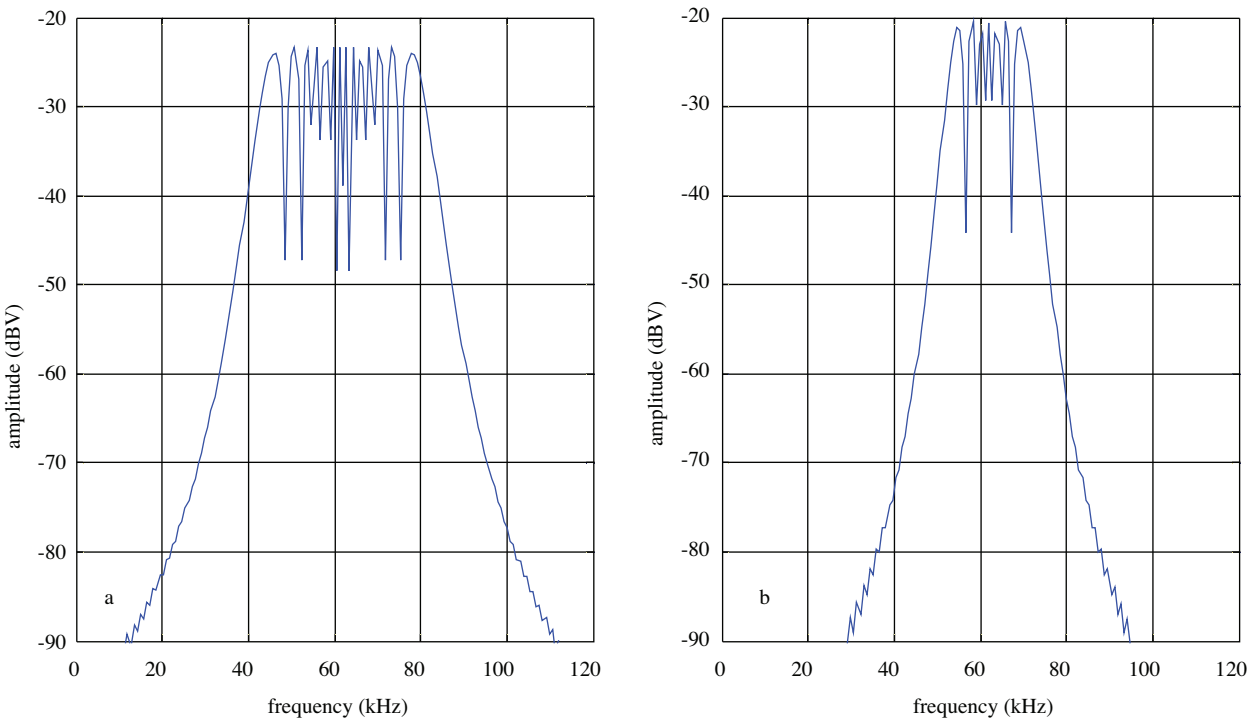

Figure 6. Spectra of FM signal modulated by triangular profile, $f_c = 62$ kHz, $f_m = 750$ Hz; a) $\Delta f_c = 20$ kHz, b) $\Delta f_c = 10$ kHz.

As shown in Figure 4, the triangular modulating profile produces a flat spectrum compared to the sinusoidal modulating signal. It also gives better amplitude reduction in the spectrum. Therefore, for the flyback converter, the triangular modulating profile was selected in the control mechanism of the switching device. Figure 5 shows that for the same modulating profile, a signal with lower frequency produces a better spectrum, whereas high-frequency deviation values result in a large reduction in the spectrum, as shown in Figure 6. This means that a higher modulation index produces larger attenuations.

The flowchart of the MATLAB algorithm used for plotting the spectra of the frequency-modulated signals is given in Figure 7. According to this, the content of the command window of MATLAB was first cleared in order to remove all variables from the workspace. The main parameters of the FM, namely f_c, f_m, Δf_c, and A_m, that are used for the computations were decided. The modulation index (β) was calculated by Eq. (8) and the bandwidth of the modulated signal was computed according to Carson's rule, using Eq. (11). The modulated waveform was defined mathematically by Eq. (9). In order to find the spectral components of the modulated signal, the *fft* function of MATLAB was used. Afterwards, the spectral components were displayed by using the *plot* command. The same algorithm was then repeated for different modulating signals.

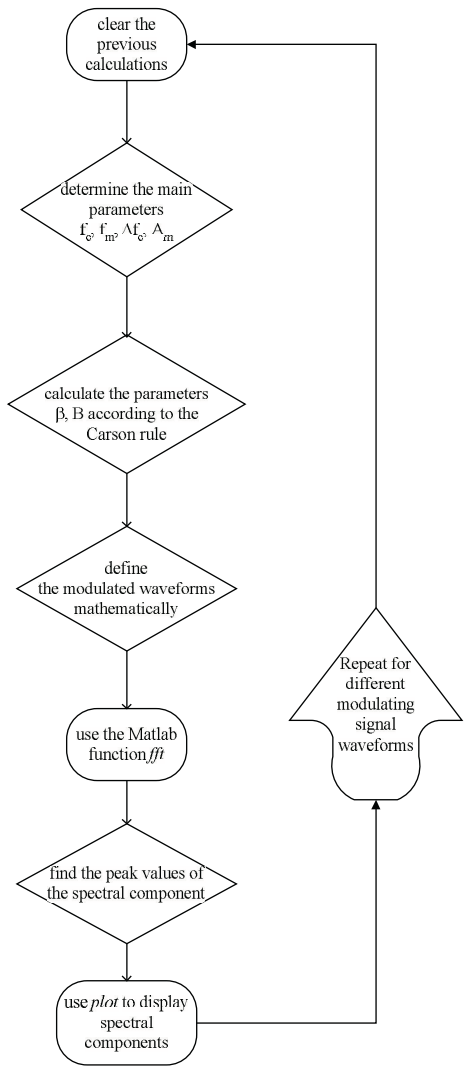

Figure 7. Flowchart of the MATLAB algorithm.

3. Realization of the AC-DC flyback converter

In order to see the effect of the FM technique on the EMI performance of the SMPS, an AC-DC flyback converter board was realized using an L6566B PWM controller chip [15]. The board accepts a wide range of input supply voltages (88-264 V AC) and delivers 12 V of DC output voltage. The general configuration of the system is shown in Figure 8.

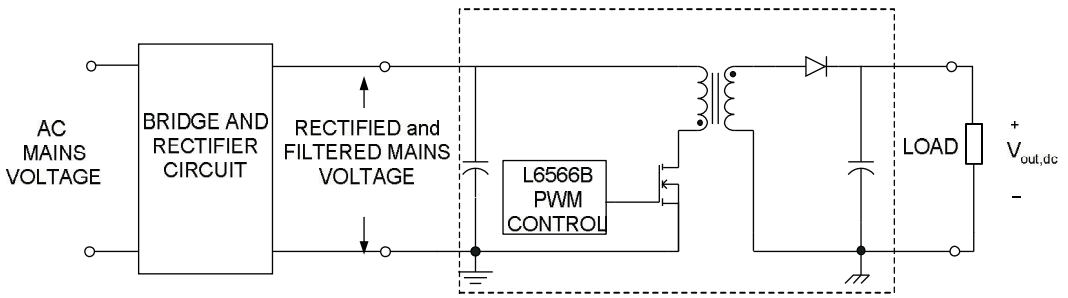

Figure 8. The general configuration of the AC-DC flyback converter.

In Figure 9, the schematic and component values of the flyback converter are given. The input of the converter is filtered by an EMI pi filter. The switching component is a standard MOSFET with a maximum of 600-V 2Ω ratings requiring a small heat sink. The transformer is a layer type that uses a standard ferrite-type EER28L. The snubber circuit, consisting of the D7, R7, and C21 elements shown in Figure 9, clamps the peak of the voltage spike on the leakage inductance. The energy stored in the leakage inductance is transferred to the capacitor C21, and when the MOSFET is on, it is dissipated on resistor R7. A Schottky diode is used as the output rectifier diode due to its low voltage drop and minimum power dissipation in comparison with the standard types. A small LC filter was added to the output terminal in order to filter the high-frequency ripple without increasing the output capacitor. The output voltage regulation is performed by feedback from the secondary to the primary side sensing the 12-V output voltage. A TL431 is used in the feedback circuit as an error amplifier. The TL431 drives an optocoupler SFH617A-4, ensuring the required insulation between the primary and secondary side of the converter. The optotransistor directly modulates the voltage on the COMP pin of the L6566B [15].

The switching frequency of the converter is determined by the value of the resistor, R_T, connected between the OSC pin and the ground. With good approximation, it is given by [15]:

$$f_c \approx \frac{2 \times 10^9}{R_T}. \tag{15}$$

The switching frequency of the converter was selected as approximately 62 kHz. The closest standard resistance value corresponding to this frequency is $R_T = 33\ \mathrm{k}\Omega$.

To improve the EMI performance of the converter, the L6566B is provided with a dedicated pin. This pin allows the designer to modulate the switching frequency and gives the possibility of selecting both the modulation frequency (f_m) and the frequency deviation (Δf_c). It is advantageous to modulate the switching frequency so that the resulting spread spectrum behavior distributes the energy of each harmonic of the switching frequency over a number of side band harmonics [15], as mentioned in Section 2.

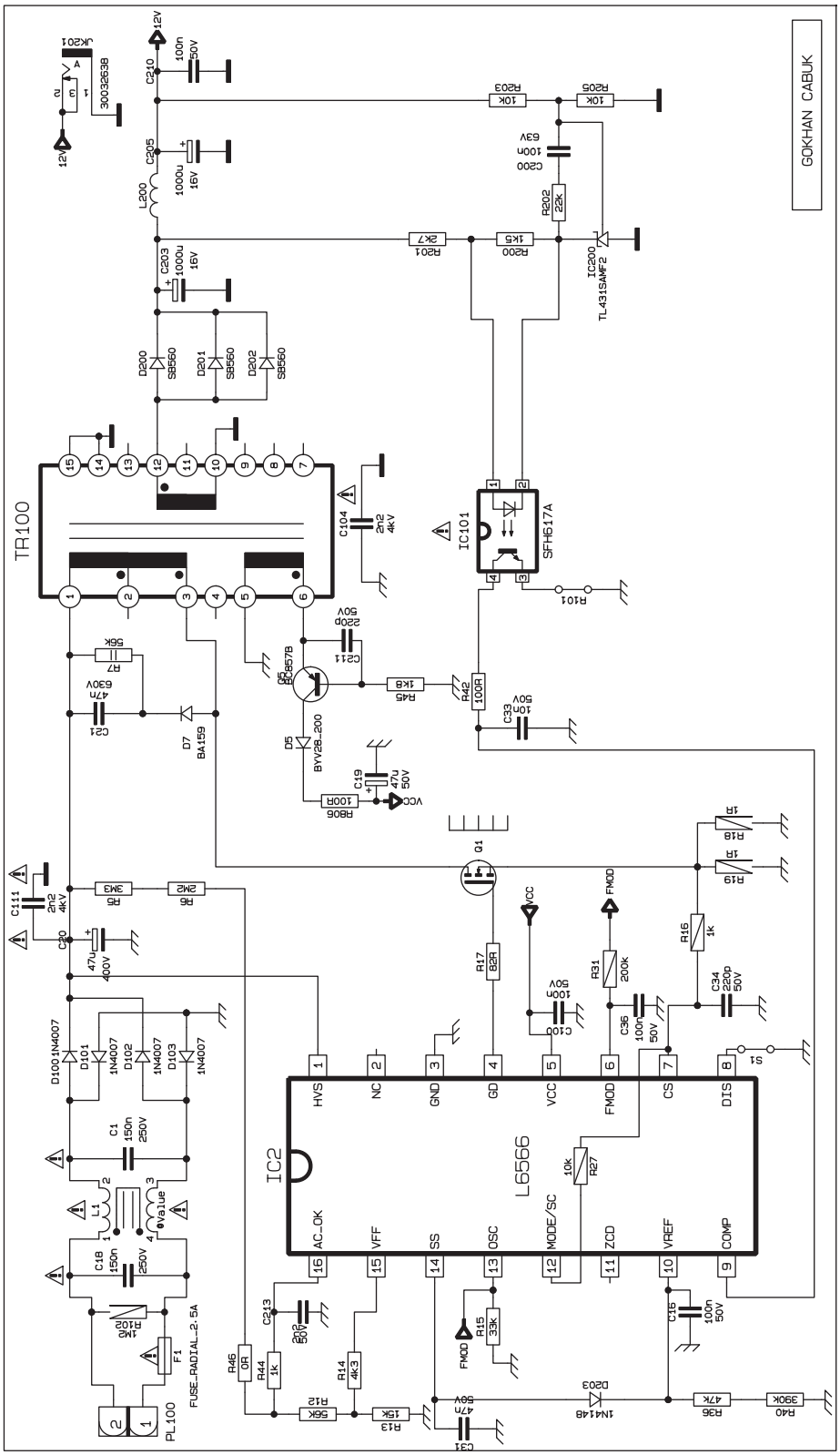

Figure 9. Circuit schematic.

As depicted in Figure 10, the capacitor, C_{MOD}, is connected between the FMOD pin and the ground and is alternately charged and discharged between 0.5 V and 1.5 V by internal current generators sourcing and sinking the same current (3 times the current defined by the resistor R_T at the OSC pin). Hence, the voltage across capacitor C_{MOD} will be a symmetric triangle, whose frequency, f_m, is determined by C_{MOD}. By connecting a resistor, R_{MOD}, between the FMOD and OSC pins, the current sourced by the OSC pin will be modulated according to a triangular profile at a frequency of f_m [15]. If R_{MOD} is considerably higher than R_T, as is normal, both f_m and the symmetry of the triangle will be slightly affected. With this arrangement, it is possible to set the frequency deviation, Δf_c, and the modulating frequency, f_m, both of which define the modulation index given by Eq. (8).

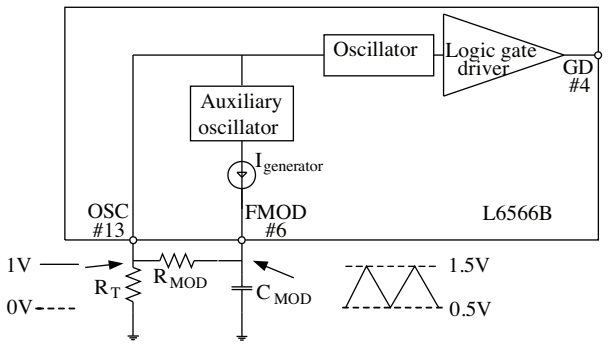

Figure 10. FM circuit of L6566B [15].

The switching frequency of the converter corresponds to the carrier frequency (f_c) in the analysis of Section 2, since the carrier for FM is the PWM signal in the present case. The maximum and minimum values of the switching frequency are directly related to the frequency deviation. The minimum switching frequency, $f_{c,min}$, which occurs at the peak of the triangle, and the maximum switching frequency, $f_{c,max}$, which occurs at the valley of the triangle, will be symmetrically placed around the center value, f_c; therefore [15]:

$$f_{c,\min} = f_c - \frac{1}{2}\Delta f_c, \tag{16}$$

$$f_{c,\max} = f_c + \frac{1}{2}\Delta f_c. \tag{17}$$

R_{MOD} and C_{MOD} can be calculated as follows [15].

$$R_{MOD} = \frac{2 \times 10^9}{\Delta f_c} \tag{18}$$

$$C_{MOD} = \frac{75 \times 10^{-6}}{f_m} \tag{19}$$

They will be selected by the designer according to circuit performance so as to achieve the best compromise between attenuation of peak EMI emissions and clean converter operation [15]. In the designed circuit, R_{MOD} and C_{MOD} correspond to R31 and C36, respectively. Different resistor and capacitor values resulting in different FM parameters were tried in order to obtain an optimal EMI spectrum, as will be explained in the next section. A photograph of the realized circuit is shown in Figure 11.

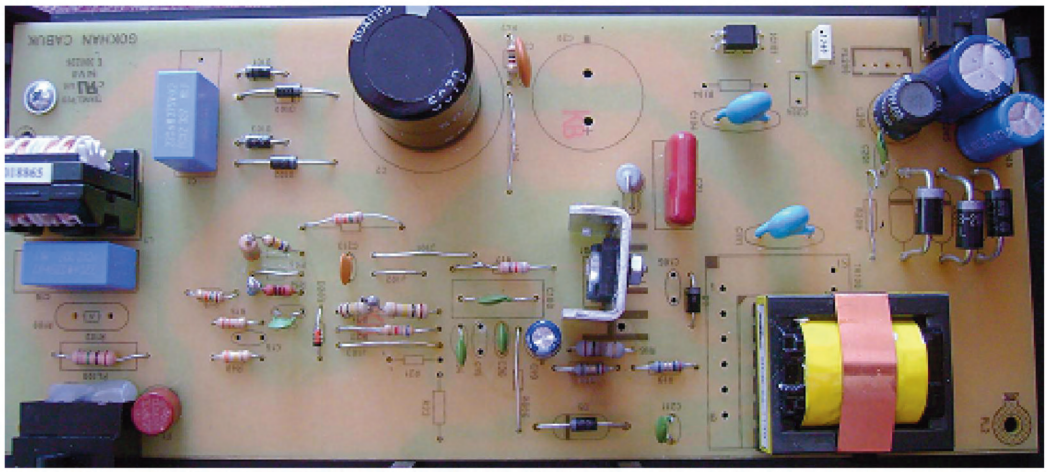

Figure 11. A photograph of the realized flyback converter.

4. Test set-up and experimental results

The test platform shown in Figure 12 was set up in order to measure the conducted emissions from the realized AC-DC flyback converter. Test results were taken between the frequencies of 150 kHz and 30 MHz, as regulated by the CISPR. A line impedance stabilization network (LISN) was inserted between the AC power cord of the device under test (DUT) and the mains power supply while testing the flyback converter. The mains power supply is filtered through the LISN, so the device's power is provided with an unpolluted AC supply. An EMI receiver is connected to the LISN, measuring the conducted emission noises from the DUT. The EMI receiver has a 9-kHz resolution bandwidth, as required by the CISPR and the relevant standards.

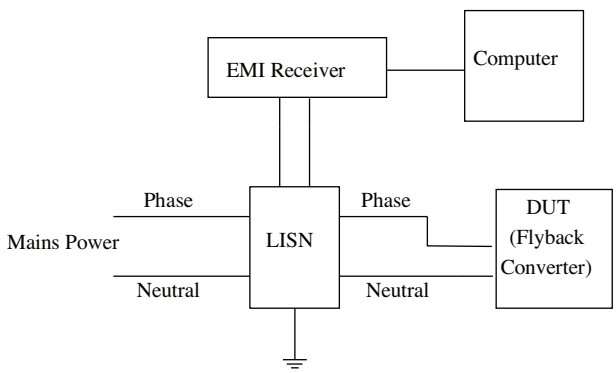

Figure 12. Diagram of the test set-up used for measuring conducted emissions.

The EMI receiver measures the signal of the EMI in the frequency domain. Both EMI receivers and spectrum analyzers actually use the same principle. The difference is that, for EMI receivers, specific parameters like the resolution bandwidth are set to a certain value obliged by the standards. They are used for full compliance measurements according to the CISPR. The data from the EMI receiver can be displayed by means of a computer. For this purpose, there is a GPIB interface card mounted in the computer. This card is used in order to establish communications between the test equipment and the computer. A GPIB cable, which has 24 pins, connects the receiver to the computer. GPIB interface protocol is determined by the standards. By using

this module, the data recorded by the receiver is converted into a form that is comprehensible for the computer. The GPIB interface also ensures that control of the EMI receiver is established by the computer.

The waveforms shown in Figures 13 and 14 were obtained for different load conditions of the flyback converter before the application of FM. From the drain current waveform in Figure 13, it is possible to conclude that the converter is working in continuous mode. This operating mode was chosen in order to optimize the values of the output filter capacitors and the ratio of the peak to the root mean square of the current flowing in the transformer windings [15]. The measured switching frequency was 63 kHz. As the load increases, the switching frequency remains the same, whereas the duty cycle of the PWM signal increases.

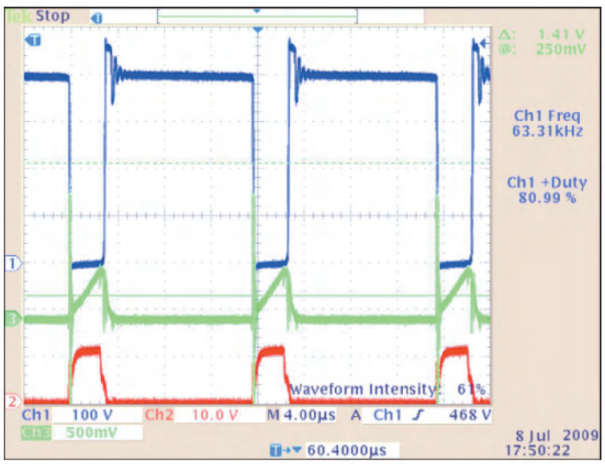

Figure 13. Waveforms for the flyback converter at 220 V AC, 50 Hz, and full load; CH1: drain voltage (100 V/div), CH2: gate voltage (10 V/div), CH3: drain current (500 mA/div) of the MOSFET.

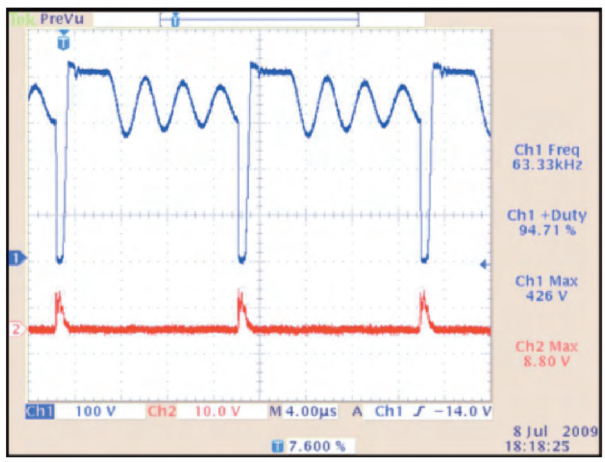

Figure 14. Waveforms for the flyback converter at 220 V AC, 50 Hz, and 4 W; CH1: drain voltage (100 V/div), CH2: gate voltage (10 V/div) of the MOSFET.

The output voltage and power of the converter measured at 220 V of AC mains supply and 1.9 A of output current were 11.83 V and 22.48 W, respectively. The measured input power of the converter was 28.27 W. Therefore, the overall efficiency was calculated as 79.52%. The output voltage and power of the converter at the 0.05-A load current were 11.99 V and 0.6 W. The efficiency of the converter was 68.49% at the measured 0.876 W of input power.

Figure 15 shows the deviation of the frequency after the FM technique was applied. The waveforms are not steady, since the frequency of these signals is changing due to the application of FM. They look like multiple graphics because their frequency is not constant and the oscilloscope could not trigger on them. The output voltage and power of the converter measured after modulation at 220 V of AC mains supply and 1.9 A of output current were 11.83 V and 22.48 W, respectively. The measured input power of the converter was 28.3 W. The overall efficiency was therefore 79.43%. The output voltage and power of the converter at the 0.05-A load current were 12 V and 0.6 W after modulation. The efficiency of the converter was 68.65% at the measured 0.874 W of input power. It is evident from these results that the converter operates properly after the FM technique is implemented; nearly the same efficiency values were obtained.

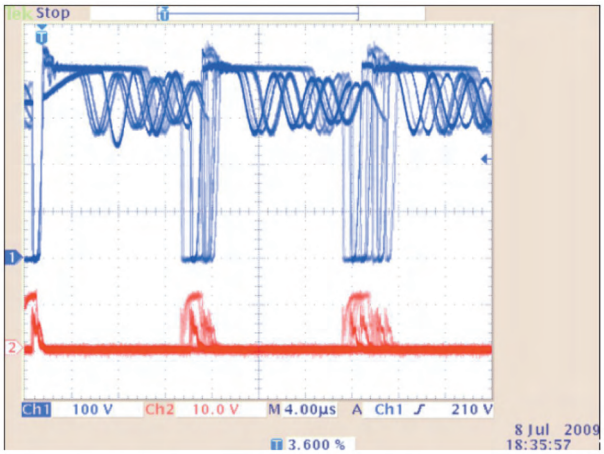

Figure 15. Drain and gate signals at light load after the application of FM (time/div: 4 μs); CH1: drain voltage (100 V/div), CH2: gate voltage (10 V/div) of the MOSFET.

For the continuous mode operation of the flyback converter, the input-output relationship can be written as [18]:

$$\frac{V_{out}}{V_{in}} = \frac{N_s}{N_p}\frac{D}{1-D}, \tag{20}$$

where N_p and N_s are the number of turns in the primary and secondary windings, respectively, and D is the duty cycle ($D \leq 1$). As seen from Eq. (20), the output voltage depends on the duty cycle of the PWM signal. It was observed from the experimental results that the duty cycle of the PWM signal remained unchanged after the FM method was applied, as was expected. Therefore, there would be no change in the amplitude of the output voltage after the implementation of the FM technique.

Figure 16 shows the experimental waveform for the fixed-frequency switching signal and its spectrum. The same graphics after the application of FM are depicted in Figure 17. As can be seen, the bandwidths of the frequency components are spread and their amplitudes are reduced by modulating the frequency of the PWM signal.

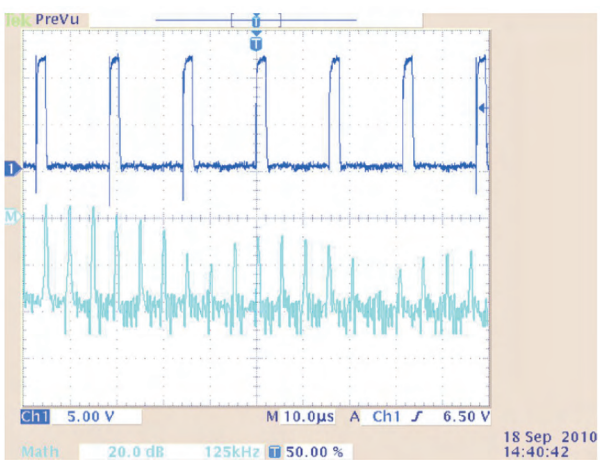

Figure 16. Fixed-frequency switching signal and its spectrum.

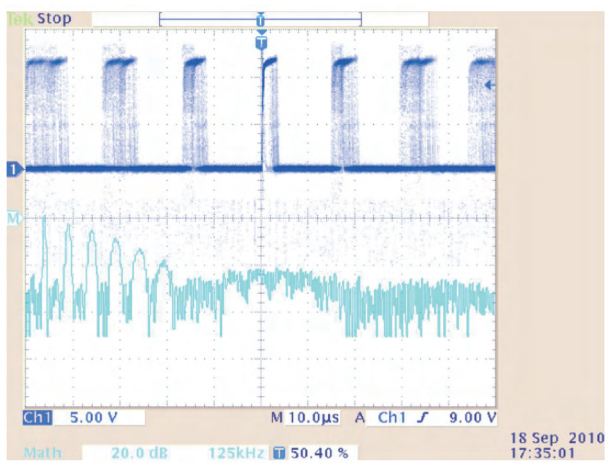

Figure 17. Switching signal after the application of FM and its spectrum.

Figures 18 and 19 show the output voltages of the converter and their spectra before and after the application of FM. It can be concluded by comparing these figures that the amplitudes of the ripples, levels of the frequency components, and hence the total harmonic distortion in the 12-V output voltage are also slightly reduced as a result of implementing the FM technique.

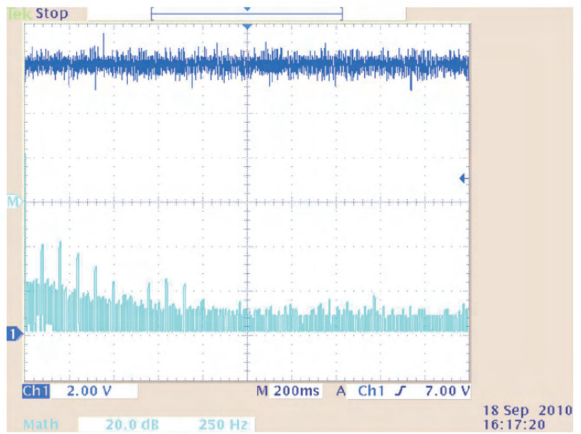

Figure 18. The 12-V output voltage of the converter and its spectrum before the application of FM.

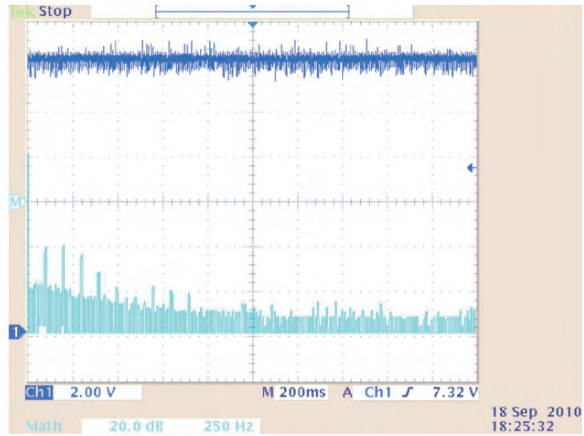

Figure 19. The 12-V output voltage of the converter and its spectrum after the application of FM.

Figure 20 shows the comparison between the EMI performances of the converter with the fixed-frequency scheme and the FM scheme. The green solid lines show the EMI measurement before modulation, at the fixed frequency, and the dashed red lines show the measurement after modulation with $R_{MOD} = 50\ \mathrm{k}\Omega$ corresponding to $\Delta f_c = 40$ kHz and $C_{MOD} = 200$ nF corresponding to $f_m = 375$ Hz. The peaks at the harmonics of the switching frequency before modulation can be easily seen here. The reduction in the noise peaks obtained by implementing the FM technique is clearly visible. The results that were taken after modulation show that there is up to 15 dBμV of attenuation at the peak values.

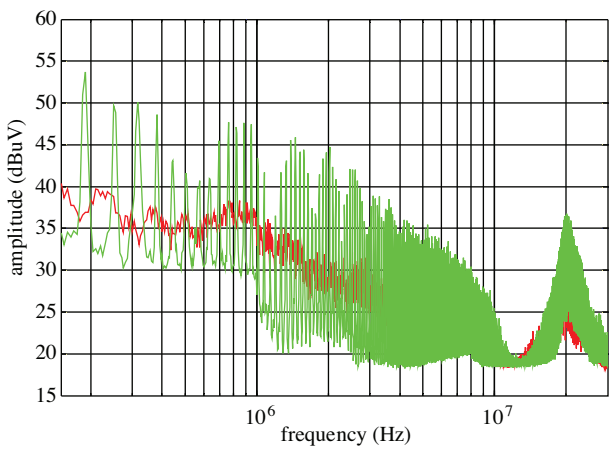

Figure 20. Comparison of the conducted noise measurements before (green) and after (red) modulation with $R_{MOD} = 50\ \mathrm{k}\Omega$ corresponding to $\Delta f_c = 40$ kHz, $C_{MOD} = 200$ nF corresponding to $f_m = 375$ Hz.

The tests were repeated for different modulating frequency (f_m) and frequency deviation (Δf_c) values, and the results are given in Figures 21 and 22. In order to obtain the best performance on the spectrum,

the R_{MOD} and C_{MOD} values were changed. Both graphics in Figure 21 were obtained for R_{MOD} = 100 kΩ corresponding to Δf_c = 20 kHz. The solid green lines in Figure 21 show the measurement with C_{MOD} = 10 nF (corresponding to f_m = 7.5 kHz), while the dashed red lines show the measurement with C_{MOD} = 200 nF (corresponding to f_m = 375 Hz). In Figure 21, it is observed that while the frequency deviation is constant (without changing the value of R_{MOD}), decreasing the f_m frequency (increment in C_{MOD}) reduces the level of the EMI noise. This confirms the MATLAB simulation results in Figure 5. The effect of the modulating frequency diminishes at higher frequencies.

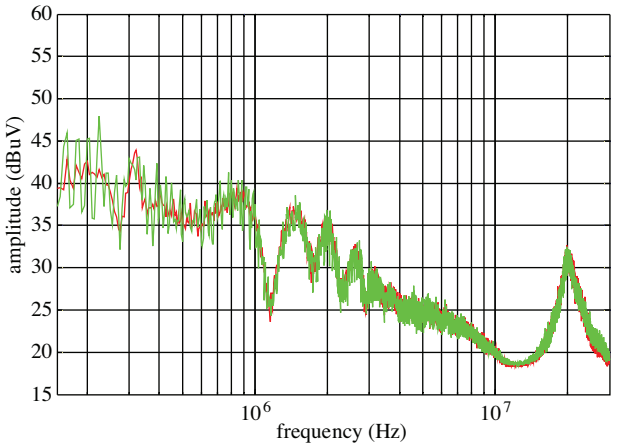

Figure 21. EMI measurements for R_{MOD} = 100 kΩ corresponding to Δf_c = 20 kHz and C_{MOD} = 10 nF corresponding to f_m = 7.5 kHz (green), C_{MOD} = 200 nF corresponding to f_m = 375 Hz (red).

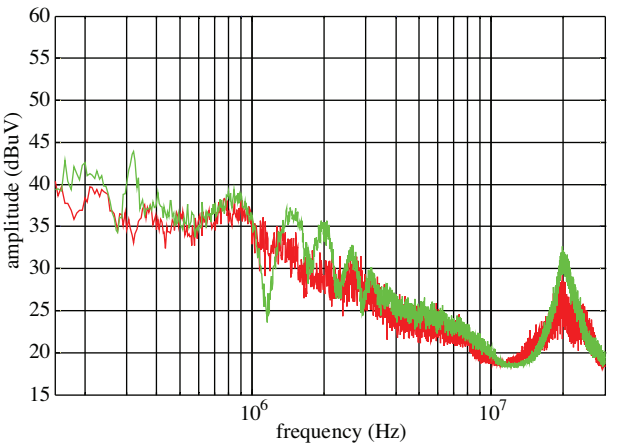

Figure 22. EMI measurements for C_{MOD} = 200 nF corresponding to f_m = 375 Hz and R_{MOD} = 100 kΩ corresponding to Δf_c = 20 kHz (green), R_{MOD} = 50 kΩ corresponding to Δf_c = 40 kHz (red).

The measurements in Figure 22 were taken at a constant f_m value (C_{MOD} = 200 nF corresponding to f_m = 375 Hz) and different frequency deviations. The solid green lines show the measurement with R_{MOD} = 100 kΩ (Δf_c = 20 kHz) and the dashed red lines show the measurement with R_{MOD} = 50 kΩ (Δf_c = 40 kHz). In Figure 22, it is observed that while the f_m frequency is constant (without changing the value of C_{MOD}), the increase in the frequency deviation (reduction in R_{MOD}) reduces the peak values of the EMI noise. This agrees with the MATLAB simulation results in Figure 6.

5. Conclusion

In this paper, the EMI performance of a flyback converter built with an L6566B integrated circuit was investigated. In order to reduce the EMI noise levels, the FM method was applied to the switching frequency of the MOSFET. The AC-DC flyback converter was physically realized and tested in the laboratory for its conducted emission performance. The effects of the modulation parameters, namely the modulating frequency (f_m) and frequency deviation (Δf_c), on the EMI spectrum were investigated by MATLAB simulations and observed by measurements. It was concluded from both MATLAB and the measurements that decreasing the f_m value reduces the level of the EMI noise, whereas the increase in Δf_c reduces the peak values of the EMI emission. The values of these parameters should be determined properly considering the operation of the converter. In terms of conducted EMI suppression, this study demonstrates that the FM scheme is better than the fixed-frequency switching scheme.

References

[1] M.H. Nagrial, A. Hellany, "Radiated and conducted EMI emissions in switch mode power supplies (SMPS): sources, causes and predictions", IEEE Multi Topic Conference, pp. 54-61, 2001.

[2] J. Kaewchai, W. Khangern, S. Nitta, "Controlling conducted EMI emission on a buck-boost converter using gate controlled circuit", International Symposium on Electromagnetic Compatibility, pp. 541-544, 2002.

[3] G. Antonini, S. Cristina, A. Orlandi, "EMC characterization of SMPS devices: circuit and radiated emissions model", IEEE Transactions on Electromagnetic Compatibility, Vol. 38, pp. 300-309, 1996.

[4] J. Balcells, D. Gonzalez, J. Gago, A. Santolaria, J.C. Le Bunetel, D. Magnon, S. Brehaut, "Frequency modulation techniques for EMI reduction in SMPS", European Conference on Power Electronics and Applications, pp. 1-8, 2005.

[5] L.H. Mweene, "How to ease EMI compliance in power converters", EE Times Design, pp. 1-2, 2006.

[6] Z.Y. He, F.Y. Shih, Y.T. Chen, Y.P. Wu, "Analysis and design of EMI filter for multi-output switching mode power supply", International Telecommunications Energy Conference, pp. 457-463, 1994.

[7] J. Paramesh, A. Von Jouanne, "Use of sigma-delta modulation to control EMI from switch-mode power supplies", IEEE Transactions on Industrial Electronics, Vol. 48, pp. 111-117, 2001.

[8] Y.C. Son, S.K. Sul, "Generalization of active filters for EMI reduction and harmonics compensation", Industry Applications Conference, Vol. 2, pp. 1209-1214, 2003.

[9] R. Bera, J. Bera, A.K. Sen, P.R. Dasgupta, "Reduction of EMI from SMPS (switched mode power supplies) by resonance technique and its utilities in industrial process control instruments", International Conference on Electromagnetic Interference and Compatibility, pp. 445-448, 1999.

[10] K. Yoshida, T. Ishii, N. Nagagata, "Zero voltage switching approach for flyback converter", International Telecommunications Energy Conference, pp. 324-329, 1992.

[11] F. Lin, D.Y. Chen, "Reduction of power supply EMI emission by switching frequency modulation", IEEE Transactions on Power Electronics, Vol. 9, pp. 132-137, 1994.

[12] K.K. Tse, H.S.H. Chung, S.Y.R. Hui, H.C. So, "A comparative study of carrier-frequency modulation techniques for conducted EMI suppression in PWM converters", IEEE Transactions on Industrial Electronics, Vol. 49, pp. 618-627, 2002.

[13] D. Gonzalez, J. Balcells, A. Santolaria, J.C. Le Bunetel, J. Gago, D. Magnon, S. Brehaut, "Conducted EMI reduction in power converters by means of periodic switching frequency modulation", IEEE Transactions on Power Electronics, Vol. 22, pp. 2271-2281, 2007.

[14] G. Çabuk, S. Kılınç, "Çapraz (flyback) çeviricilerde frekans modülasyonu tekniği kullanılarak elektromanyetik girişimlerin azaltılması" (in Turkish), Electrical, Electronics, Computer and Biomedical Engineering National Congress, pp. 207-212, 2009.

[15] L6566B Multi-Mode Controller for SMPS, Data Sheet, ST Microelectronics, 2008.

[16] S. Haykin, Communication Systems, New York, John Wiley & Sons, 1994.

[17] J.R. Carson, "Notes on the theory of modulation", Proc. IRE, Vol. 10, pp. 57-54, 1922.

[18] Y.S. Lee, Computer-Aided Analysis and Design of Switch-Mode Power Supplies, New York, Marcel-Dekker, 1993.